Global Journal of Earth and Environmental Science
Volume 5(3), pages 58-72, August 2020
Article Number: 589282361
ISSN: 2636-6002
https://doi.org/10.31248/GJEES2020.075
https://integrityresjournals.org/journal/GJEES
Full Length Research

Polyphasic tectonic history of the N70° DASA Graben (northern, Niger)

Abdoulwahid Sani[1*], Moussa Konaté[1], Dia Hantchi Karimou[2] and Peter Wollenberg[3]

[1]Department of Geology, Abdou Moumouni University, P. O. Box 10662, Niamey, Niger.
[2]Department of Geology, Dandicko Danklodo University, P.O. Box 465, Maradi, Niger.
[3]Global Atomic Corporation, Toronto, Canada.

*Corresponding author. Email: awahidsani@yahoo.fr; Tel: (+227) 96900925.

Received 30th June, 2020; Accepted 6th August, 2020

ABSTRACT: Located in northern Niger, the N70° DASA graben is a trough discovered recently in the Tim Mersoï basin. In this study, a tectonic history of the DASA graben was presented based on the combined use of satellite imagery, field observations and measures, available literature and borehole data. These data were used to analyse the sedimentary facies and the tectonic deformations in the DASA graben, and derive their relative chronology. For this purpose, uplift and rift deformations and their interactions with sedimentation were characterized. Overall, the analyses suggest that the DASA graben was affected from the Carboniferous to the Cretaceous by three major tectonic phases: the first phase was an uplifting stage with extension during the Carboniferous to Permian; the second phase was a rifting stage. The mean extension was ~ N160° and dominantly produced ENE-WSW trending normal faults; and the third phase was a postrift stage. It was characterized by a ~ N130° compression. The structural and sedimentological features defined the DASA graben as a particular type of syn-sedimentary basin evolving from a transpressive tectonic regime during the period ranging from Carboniferous to Permian to an extensive tectonic regime during the period ranging from Triassic to Lower Cretaceous. Thus, the second period marked by an extensional regime would probably be related to the initial stage of the opening of the Atlantic Ocean. After this rifting period, the DASA graben was affected by a compressional phase related to the collision between Africa and Europe.

Keywords: Compression, DASA graben, extension, geodynamic model, north Niger, tectono-sedimentary evolution, rifting, uplift.

INTRODUCTION

The Paleo-Mesozoic Tim Mersoï basin is located in the northeastern part of the Iullemmeden basin and limited to the East by the Aïr Mountains (Figure 1). According to Moussa (1992), the Tim Mersoï basin infilling thickness is about 1,800 m. The detrital material was deposited during the period ranging from Devonian (410 Ma) to Lower Cretaceous (96 Ma) (Billon, 2014). This basin, located on a stable lithosphere, may provide a very good example of an intracratonic basin with a low average subsidence rate preserved over a long period (Gerbeaud, 2006; Mamadou, 2016).

During several years, the Tim Mersoï basin has been the subject of uranium exploration and exploitation campaigns. In recent campaigns of mineral exploration, the N70° trending graben of DASA (Dajy Surface Anomaly) has been discovered approximately 120 km from the town of Agadez (Figure 1). Logging data indicate that DASA graben sediment infilling is predominantly from Carboniferous (345 Ma) to Lower Cretaceous (99 Ma) which implies a sedimentation duration of 246 Ma. The maximum thickness of the DASA graben deposits is estimated at 850 m, implying an average of subsidence

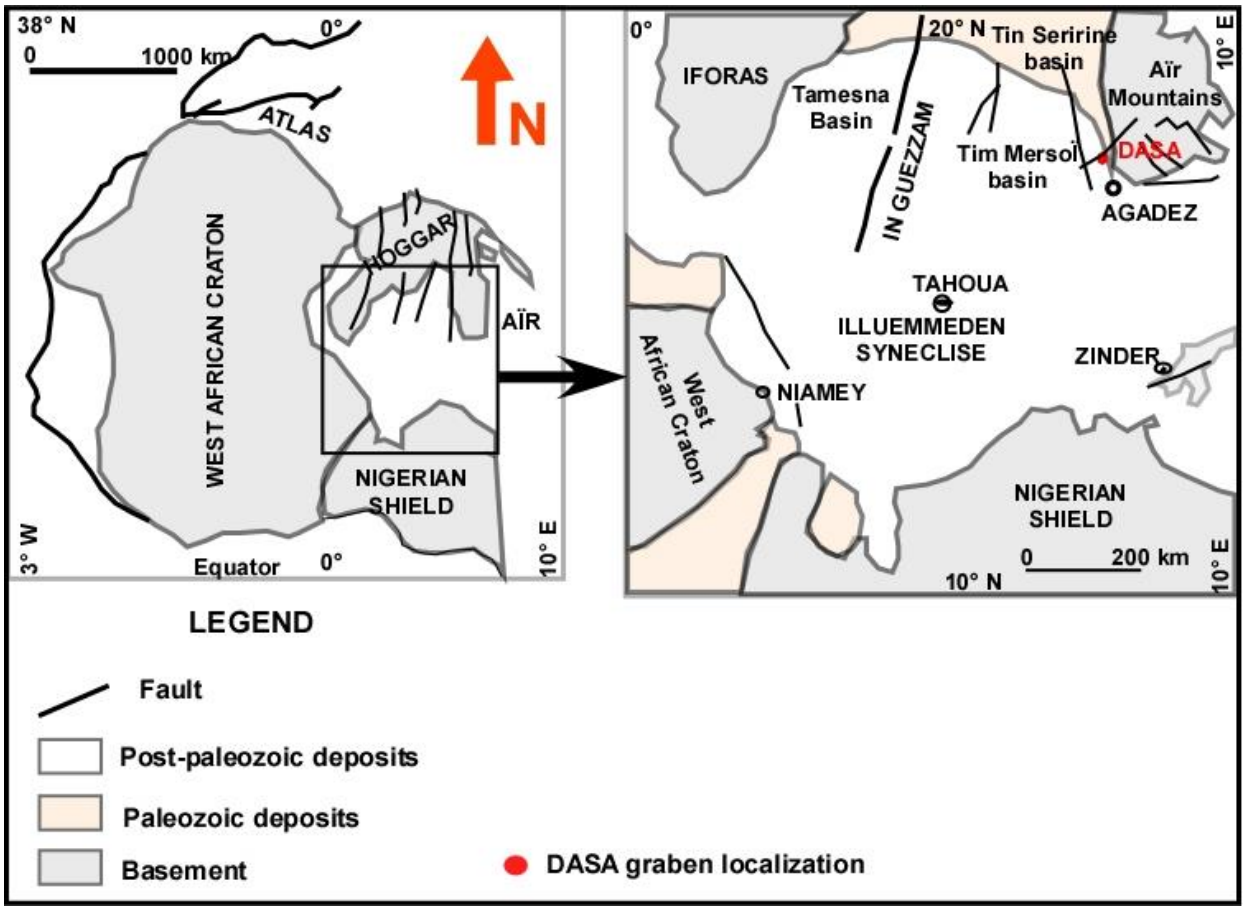

Figure 1. Geographical location of the Tim Mersoï Basin in the Iullemmeden syneclise (Konaté et al., 2007, modified).

rate of approximately 3.46 m/Ma. In the rest of the Tim Mersoï basin, for the same period, the thickness of the deposits is estimated at 1,400 m (Moussa, 1992; Konaté et al., 2007). Indeed, for the period ranging from the Carboniferous to the Lower Cretaceous (246 Ma), the maximum thickness of the Tim Mersoï basin deposits is approximately 1,400 m (Forbes, 1989).

Therefore, for the same period, the mean subsidence rate of Tim Mersoï Basin is about 5.69 m/Ma. Thus, comparatively to the Tim Mersoï basin, the DASA graben, which is its sub-basin, has paradoxically a lower subsidence rate. Theoretically, a strong subsidence rate in the graben should be expected, assuming the addition of additional tectonic subsidence related to the normal faulting. Hence, the difference in the subsidence rate of the DASA graben raises questions about the mechanisms or factors causing the subsidence.

The purpose of this article is to provide an overview of the mechanisms or factors that explain the overall reduction of DASA graben collapse, while allowing the reconstruction of tectono-sedimentary history. Concerning the sedimentary infilling, emphasis is placed on the outcropping series, generally represented by Lower Cretaceous formations in the graben, and particularly on the Jurassic age series along the edges of the graben. On the other hand, the basal series, Carboniferous to Triassic, do not outcrop. Then, the tectono-sedimentary study requires the use of appropriate methods to access subsurface information. To answer all these questions, a multidisciplinary approach adopted by integrating geological mapping, borehole and well log data analysis and microtectonic analysis. In a specific way, it involves:

1. a structural analysis that will allow to characterize Jurassic and Cretaceous tectonic events;
2. a characterization of the syn-sedimentary tectonics markers; and
3. to establish a geodynamic model for the DASA graben infilling.

GEOLOGICAL SETTING

The Paleo-Mesozoic Tim Mersoï basin geological history

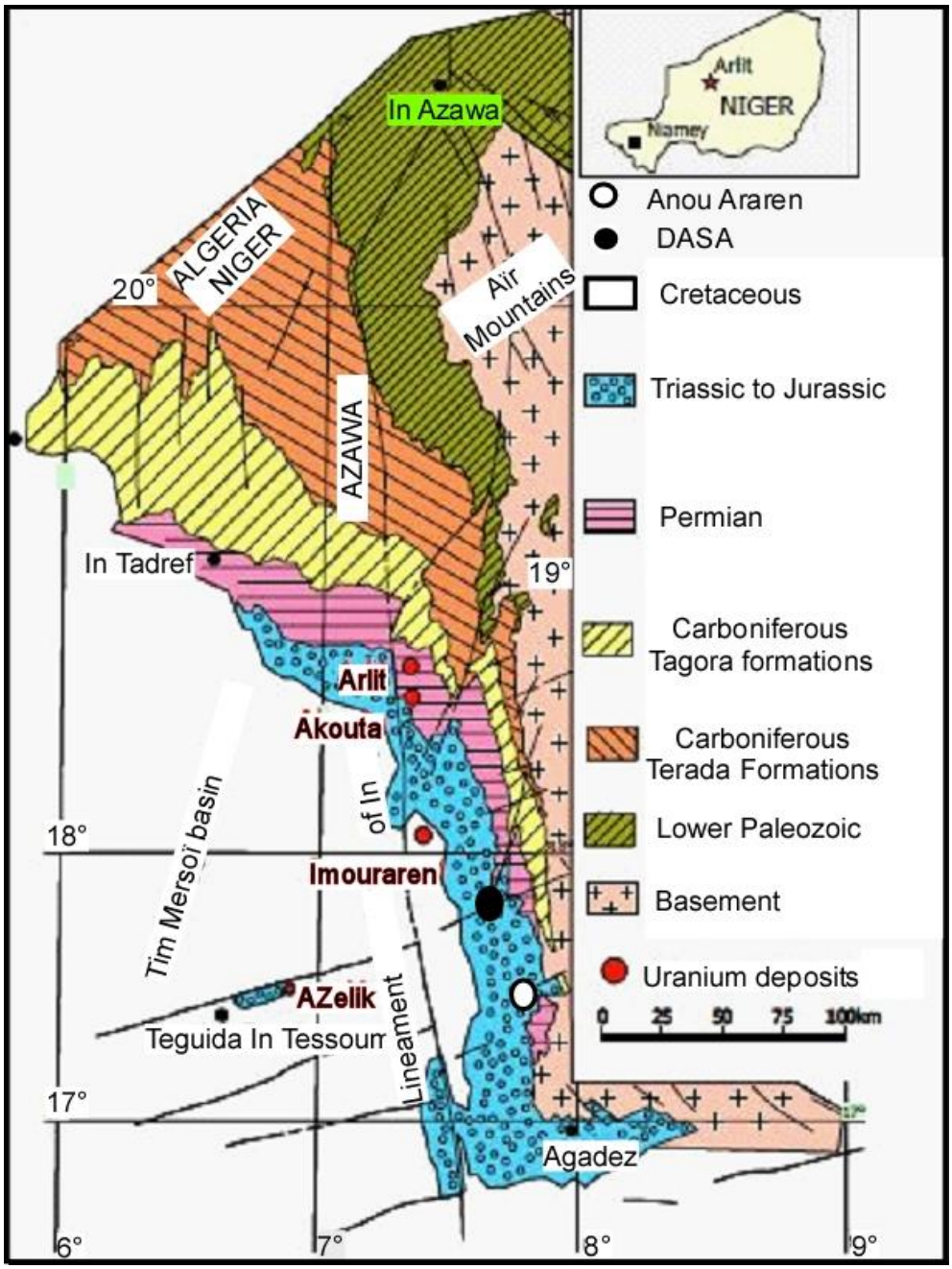

Figure 2. Simplified geological map of the Eastern part of the Tim Mersoï Basin (COGEMA, 2006, modified).

begins as early as the Cambrian in the Tin Séririne Syncline (Joulia, 1959). Subsequently, the sedimentation areas moved southward, resulting in the deposition of continental and marginal-littoral detrital formations ranging from Cambrian to Oligocene (Figure 2). Along the western edge of the Aïr Mountains, these detrital formations exhibit stratigraphic bevels from the Devonian to the Jurassic (Clermonté et al., 1991). The Tim Mersoï basin is characterized by a sedimentary infilling, resting unconformably on the Precambrian basement (Figure 2). The basin was infilled during three successive cycles including: Carboniferous cycle, Permo-Triassic to Jurassic one and Lower Cretaceous.

The first sedimentary cycle is characterized by the continental shelf facies, directly delivered from the NE from the Aïr Mountains while the second, also platform-

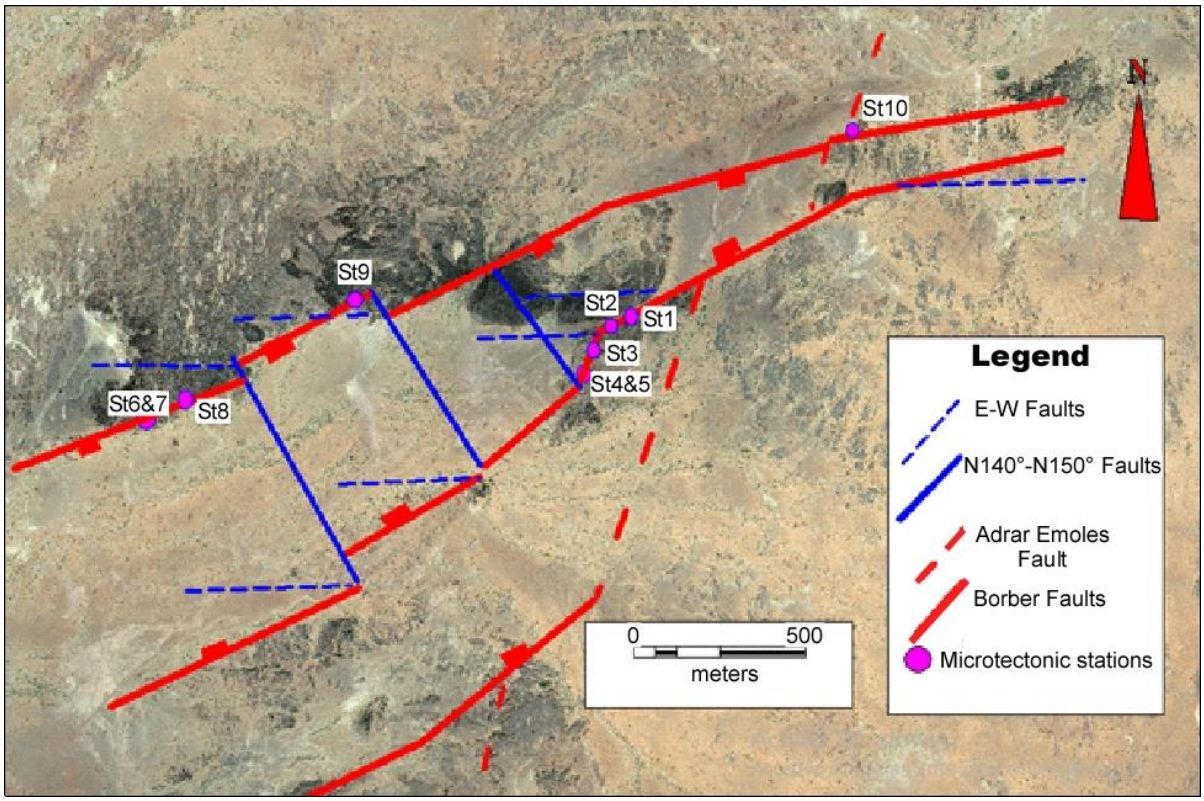

Figure 3. DASA graben.

dominated, received contributions from the SSW. The third cycle is represented by a clayey to sandy-clayey floodplain extending from the west to the center of the previous deposition area, which was gradually uprising in size (Forbes 1989; Clermonté et al., 1991).

According to Tauzin (1981), several deformations affect the sedimentary infilling. These reflect the attenuation in the sedimentary deposits of the setback sets of the underlying basement. Three main directions of faults have been highlighted (Figure 3):

1. The N0° trending lineament of In-Azaoua-Arlit and the N30° trending fault system of Madaouéla. All of exploited uranium deposits are located on the eastern compartment of the Arlit fault, but uranium deposits have also recently been discovered in the western compartment (Mamadou, 2016). The Madaouéla N30° fault system express in the basement and in the sedimentary cover in the form of flexure. These accidents are spaced twenty kilometers apart. The most important are the Madaouéla (sector of Arlit) and Adrar-Emoles (sector of DASA) trending faults.
2. The N130° to N140° trending faults represent the main fault system that affect the Aïr Mountain. In the sedimentary series, these directions are not well expressed. The Arlit fault is associated with several N150° striking faults in the Arlit mining area (Mamadou, 2016).
3. The N70° to N80° trending faults crosscut the basement intensively and also spread into the sedimentary deposits. The N70° trending faults are reactivated in dextral strike-slip movement during the upper Cretaceous (Guiraud et al., 1981). At the regional scale, the N70° trending faults network plays a fault-damping role on the N30° faults (Gerbeaud, 2006).

The DASA graben is located within the Adrar Emoles 3, claim block in the Eastern part of the Azelik Dome. Adrar Emoles 3 covers an area of 121.3 km^2. It is located between latitudes 7°40'00" and 7°53'00" and longitudes 17°51'14" and 17°45'30". From a stratigraphic point of view, all known sedimentary series in the Tim Mersoï basin are well represented in DASA area. These are Carboniferous, Permian, Triassic, Jurassic and Cretaceous series (Figure 2). The main faults observed in the DASA graben are: Azouza fault which marked the border of the graben, Adrar-Emoles N30° striking fault and secondary faults N130° to N150° trending and E-W striking (Figure 3). The DASA graben has the same orientation as the Carboniferous coal trough of the Anou Araren region (Figure 2).

These coal troughs are limited by two major N70° trending dextral strike-slip faults. These are the Isokenwali fault in the northern part and the Aboye one in the Southern part. These two faults belong to the same system as the Tin Adrar N70° striking fault system, which is well represented in the Arlit region (Wright, 1989). Most of works carried out in the Tim Mersoï basin so far have focused on the tectono-sedimentary evolution of the basin and the uranium metallogeny (Greigert, et al., 1967; Valsardieu, 1971; Sempéré, 1981; El hamet, 1983, Forbes, 1989, Moussa, 1992; Wagani, 2007; Konate et al., 2007; Mamadou, 2016). However, the troughs formed in Tim Mersoï basin have been scarcely studied (Guiraud, 1981; Konaté et al., 2007).

METHODOLOGY

A multidisciplinary approach has been implemented in this study. It is based on:

1. Geological mapping of the DASA sector, based on the combined use of satellite imagery and field observations. According to satellite imagery, it was obtained by high-resolution three-dimensional laser scanning (LIDAR). The specifications of the coordinate system used are: Ellipsoid and reference system: WGS84 and Projection: UTM32 North. Aircraft used: Diamond DA42 MPP, Laser scanner used: Leica ALS50-II and a camera: 39 megapixels Leica RCD105 with a 60 mm lens. Ten sections were made along the axis of the DASA graben and seven other sections are disposed perpendicularly to the axis of the graben. The use of the MapInfo software enabled to correlate the data collected, resulting in the geological map of the DASA sector.
2. Tectono-sedimentary analysis, based on cores drilling, cross sections and well log data analysis. In the DASA area more than 1,000 boreholes were carried out. Some of these borehole data have been used to perform a model of the structural evolution of the DASA graben. Thus, the cross-sections disposed perpendicularly to the DASA graben axis allow to observe its tectono-sedimentary evolution during the main period of infilling (Carboniferous, Permian, Triassic, Jurassic and Early Cretaceous).
3. To conduct the microtectonic analysis, satellite imagery the locations where outcrops are well preserved were chosen. Thus, ten (10) locations were chosen along the edge of the DASA graben. Each microtectonic place is characterized by a population of microfaults including 10 to 15 measurements. Nearly 136 striated microfault planes were analyzed. For each striated microfault plane measured, the following characteristics were collected: (i) direction (0-180°) and dip (0-90°) of the microfault planes; (ii) pitch of the striae (0-90°) and its plunging area (0-180°); (iii) direction of displacement of the microfault plane (N for normal, I for inverse, D for dextral and S for sinistral); (iv) reference number for striated plane measured.

Thus, the measurements obtained make it possible to establish a data file according to the model of Table 1. The different populations of microfault planes were analyzed by using Win tensor program (Damien, 2019).

RESULTS

Geological mapping

Most of the previous mapping in the Tim Mersoï basin has been restricted to the Arlit area, which was of special uranium mining interest. In the areas previously considered to be of lower uranium potential, such as the DASA sector, no detailed tectono-sedimentary analysis has been conducted so far. In the DASA area, the only maps available are those of Joulia (1963) at a scale of 1:500000 and PNC (1987) at a scale of 1:50000. These maps present uncorrelated informations; for example, the same facies have been mapped and interpreted differently according to the different authors. These observations also apply to the identification and the interpretation of brittle structures and for the determination of their kinematics. To overcome this lack of concordance, map data were supplemented by field data. This approach made it possible to update the geological map of the DASA area at a scale of 1:50000 (Figure 4). The mapped area extends over a length of 10 km and a width of 3 km. Seventeen cross-sections were made. Seven of them are parallel to the N70° axis of the graben, and the ten others are disposed perpendicularly to its axis. The outcropping sedimentary formations at the DASA sector range from the Permian to the Lower Cretaceous. These are the formations of Moradi, Téloua, Mousseden, Tchirezrine 1, Abinky, Tchirezrine 2, Irhazer and Tégama (Figure 4). The DASA graben is affected by two major faults, the N70° trending Azouza fault and the N30° Adrar Emoles fault (Figures 3, 4 and 7).

Petrographic features of the outcropping sedimentary formations of DASA sector

The outcropping sedimentary formations of the DASA sector are:

1. Moradi formation: It's mostly composed of reddish carbonated mudstones and arkosic analcime-rich coarse-grained sandstones, including intercalations of greyish carbonated siltstones.
2. Téloua formation: This formation consists of conglomerates, fine-grained sandstones and Arkosic grained sandstones with analcime.

Table 1. Example of microtectonic data file.

Microfault plan of station No 2		Dip	Striae pitch	Movement
No	**Direction**			
1	70°	46°N	75°N	Normal
2	70°	52°N	65°N	Normal
3	73°	55°N	75°N	Normal
4	75°	45°N	72°N	Normal
5	68°	55°N	70°N	Normal
6	75°	47°N	65°N	Normal
7	76°	40°N	50°N	Normal
8	88°	74°N	55°N	Normal
9	90°	75°N	50°N	Normal
10	72°	55°N	45°N	Normal
11	76°	48°N	60°N	Normal
12	78°	25°N	55°N	Normal
13	74°	20°N	55°N	Normal

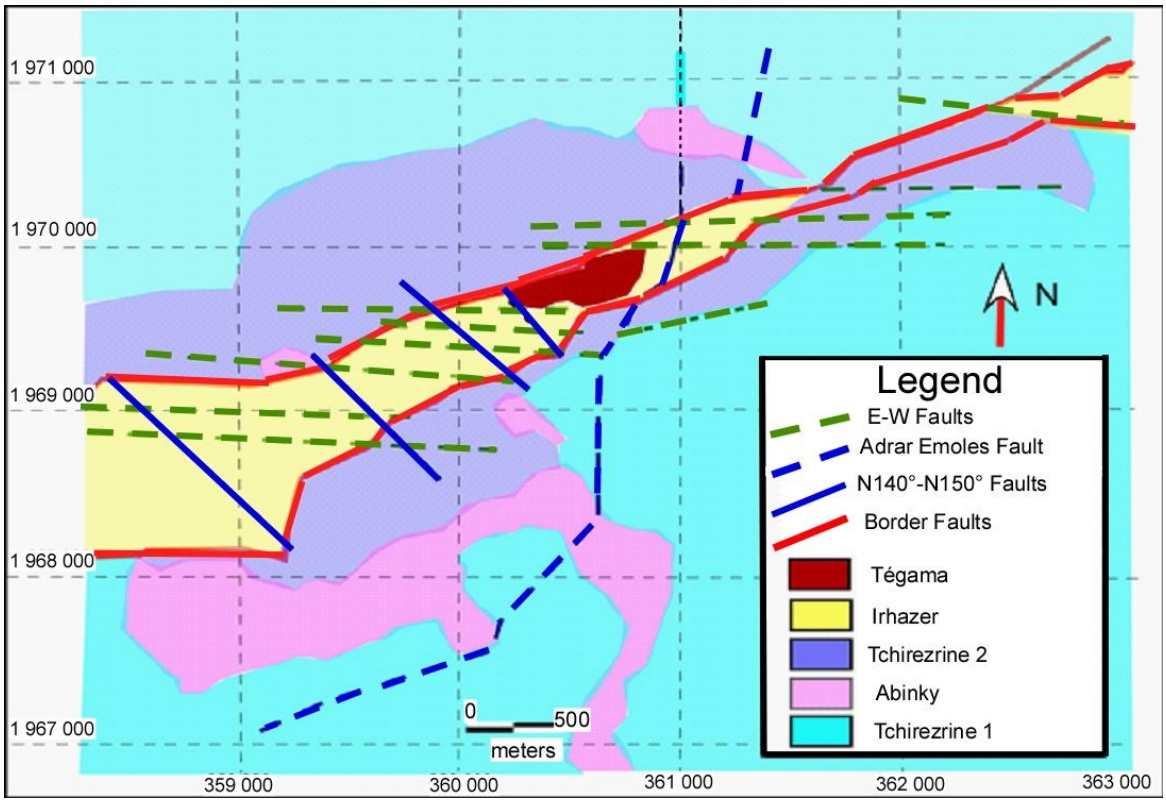

Figure 4. Geological Map of DASA Sector.

3. Mousseden formation: It consists of medium to fine grained sandstone enriched with analcimolites.
4. Tchirezrine 1 formation: It composed of Arkosic coarse grained sandstones with analcimolitic horizons.
5. Abinky formation: This formation corresponds to massive analcimolites.
6. Tchirezrine 2 formation: Correspond to coarse grained sandstones intercalated with analcimolitic horizons.
7. Irhazer formation: Red carbonated mudstones intercalated with siltstones and rarely calcareous.
8. Tégama formation: It consists of fine to medium grained sandstones.

Tectono-sedimentary analysis

To better understand the DASA graben structuration,

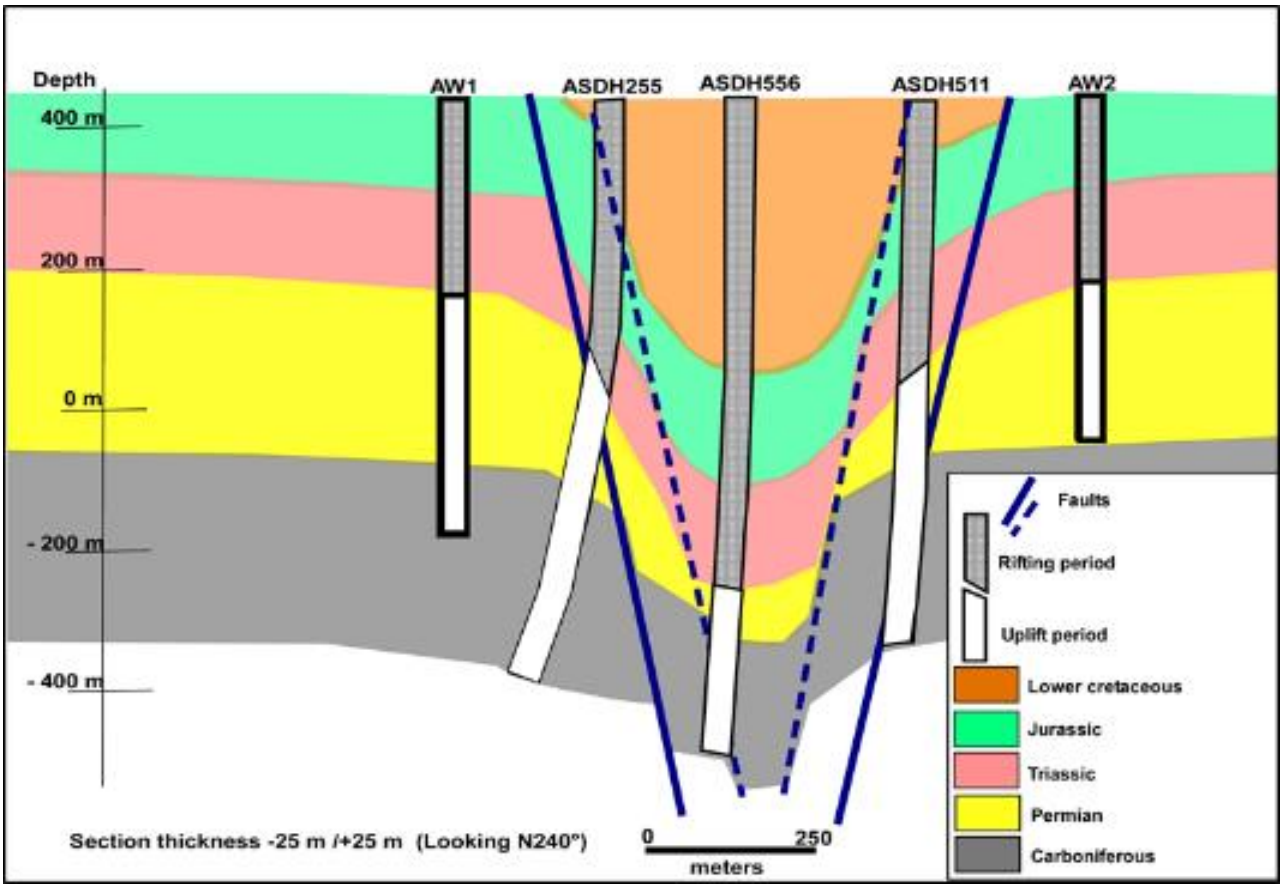

Figure 5. Geological section of the DASA graben made from survey data.

synthetic cross-sections from well logs correlation (Figures 3 and 5) were constructed. This approach allowed showing the lateral and vertical succession of the different facies and precising the relationships between tectonics and sedimentation (Figure 5). The geological section obtained shows that in the axial zone of the DASA graben, the maximum thickness of the sediment is about 805 m, over a sedimentation period of 246 Ma. This implies a lower mean subsidence rate (3.46 m/Ma) (Figure 5) compared to the Tim Mersoï basin for which the average subsidence rate is in the order of 5.69 m/Ma (Figure 6). Most of sedimentary series of the DASA graben exhibit variations in thickness on both sides of the border faults (Figure 5). However, these variations in thickness are more or less marked according to the stratigraphic series (Table 2).

The sedimentary infilling of the DASA graben is characterized by two periods of subsidence:

1. A first period with a lower subsidence rate (3.75 m/Ma on average), which extends from the Carboniferous to the Permian. The Permian series are particularly characterized by large reduction in thickness in the axial zone of the graben (30 m), compared to the edge zones (188 to 215 m) (Figure 5).
2. A second period marked by a strong subsidence rate (4.11 m/Ma) from the Triassic to the Lower Cretaceous (Figure 5). The strongest subsidence rate occurred during the Lower Cretaceous in the axial zone (6.52 m/Ma) while in the border zones the subsidence rate is very low (1.17 to 1.65 m/Ma) (Figure 5).

These lateral variations of subsidence and thickness highlight a syn-sedimentary tectonic activity preserved over a long period from the Carboniferous to the Lower Cretaceous. The subsidence inversions between the axial zone of the DASA graben and its borders reflect a morphological inversion related to a change in the tectonic regime.

During the first period from the Carboniferous to the Permian, the axial zone of the DASA graben was affected by an uplift stage. The latter induced a reduced thickness of the Carboniferous and the Permian series in the axial zone of the graben, in connection with a reduction of the available space. The axial zone of the graben would then correspond to a paleo-high with respect to the collapsed border areas. This paleo-high would have prevailed from

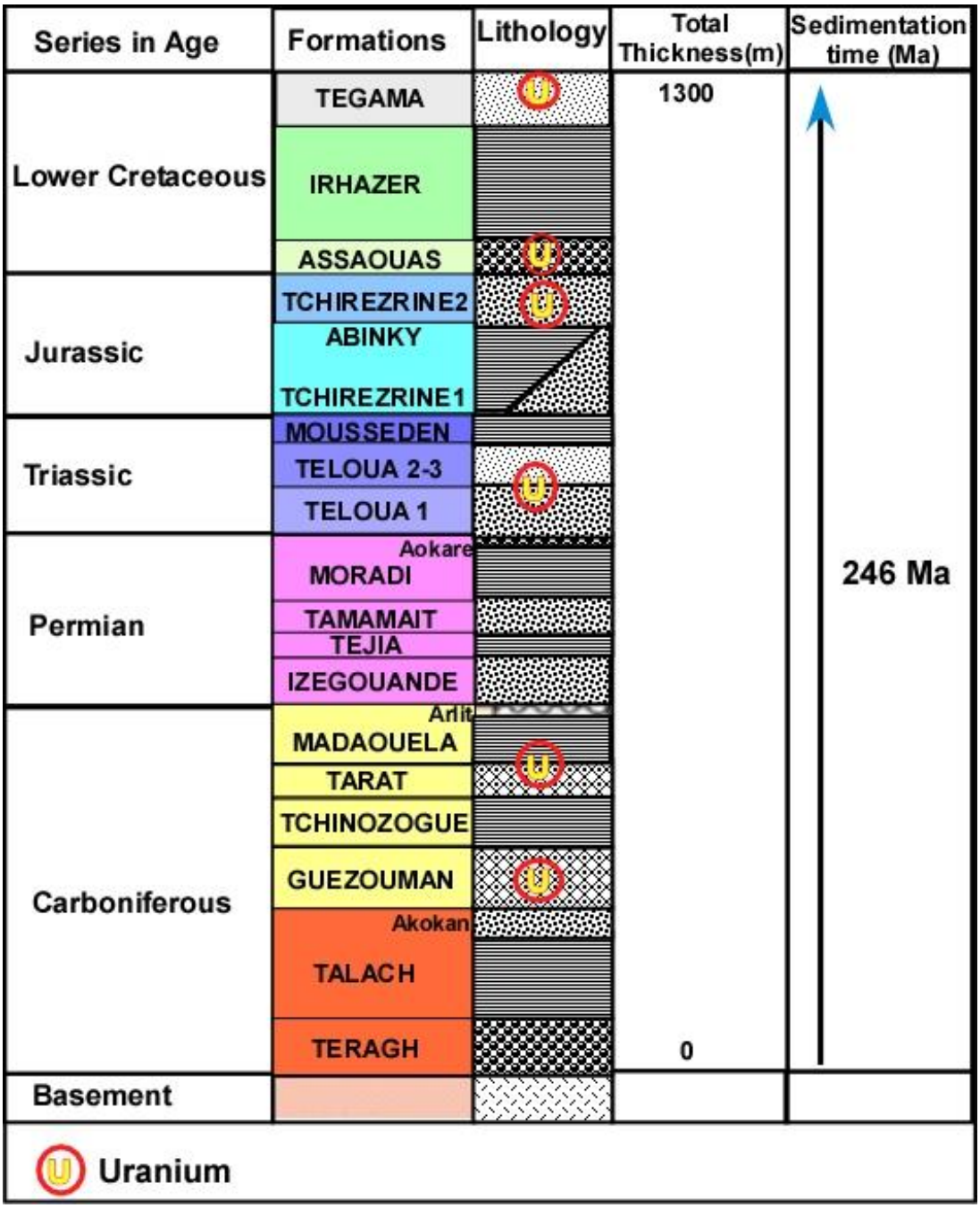

Figure 6. Simplified stratigraphic log of the geological series of the Tim Mersoï basin (Cazoulat, 1984, modified), mean subsidence = 5.69 m/Ma.

the Carboniferous to the Permian.

During the second period, from the Triassic to the Lower Cretaceous, the largest thickness of the deposits is observed in the axial zone of the graben while the thicknesses are lower within the border zones.

The DASA graben would have acquired its "actual" geometry preserved from the Triassic to the Lower Cretaceous. Three successive episodes of rifting marked this second period:

1. A first episode of Triassic rifting favorizes an increase in the available space in the axial zone. This is explained by a stronger thickening of the Triassic series in the axial zone (145 m) compared to the

Table 2. Thickness of sedimentary series at level of DASA graben.

Sedimentary series	NW area (AW2 and ASDH511) in m	Centrale area (Survey ASDH556) in m	SE area (ASDH255 and AW1) in m
Lower cretaceous	76	300	54
Jurassic	160	180	154
Triassic	112	145	126
Permian	215	30	188
Carboniferous	206	150	190
Total thickness	786	805	698

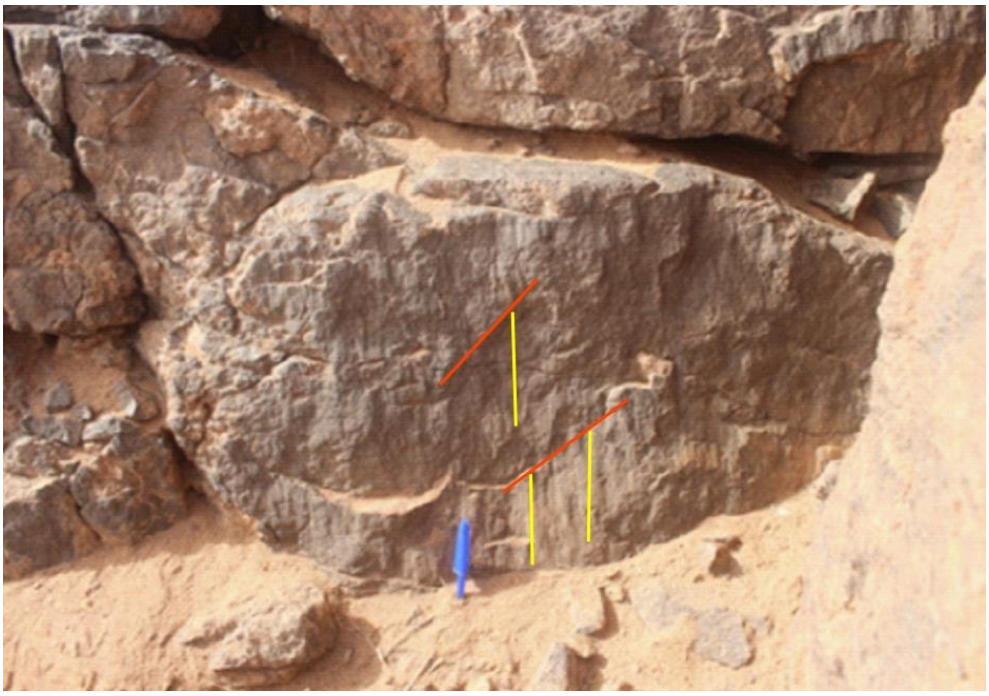

Figure 7. Normal microfault plane with fluted striaes (observed in Tchirezrine 2 sandstones), the lunules indicate that it is a normal fault. In yellow the first generation striation and in red the second generation striation.

border zones (112 to 126 m) (Figure 5).

2. A second episode of Jurassic rifting presents the same characteristics as the latter one. The highest thicknesses (180 m) are observed in the DASA graben, whereas the border zones display a reduced thickness (154 to 160 m).
3. The third episode of rifting, corresponding to the Lower Cretaceous, is marked by a considerable thickness in the axial zone (approximately 300 m) compared to the border zones (54 to 76 m) (Figure 5). The Lower Cretaceous appears to be the highest subsidence episode at the DASA graben scale, indicating strong tectonic activity.

The succession of uplifting and rifting periods confirms the change in the tectonic regime mentioned earlier. This inversion occurs at the Permian/Triassic boundary.

After the rifting phase, the DASA graben was affected by a post-cretaceous compressive phase. This compressive phase (~N130°) (Gerbeaud, 2006) is well documented in the Tim Mersoï basin. In the DASA graben, this compression phase was evidenced by the crossing of striations as observed on fault planes, where first-generation striations are intersected by second-generation striations (Figure 7).

Syn-deposition microfaults analysis

In the DASA graben, Paleo-Mesozoic sedimentary

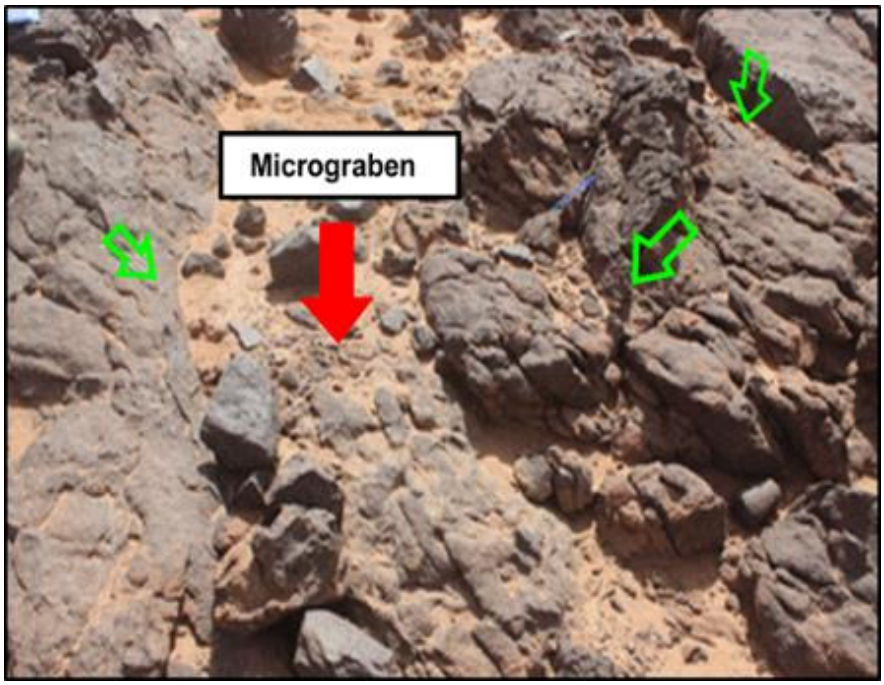

Figure 8. Secondary micrograben affecting Jurassic sandstones of the Tchirezrine 2 formation in the DASA graben.

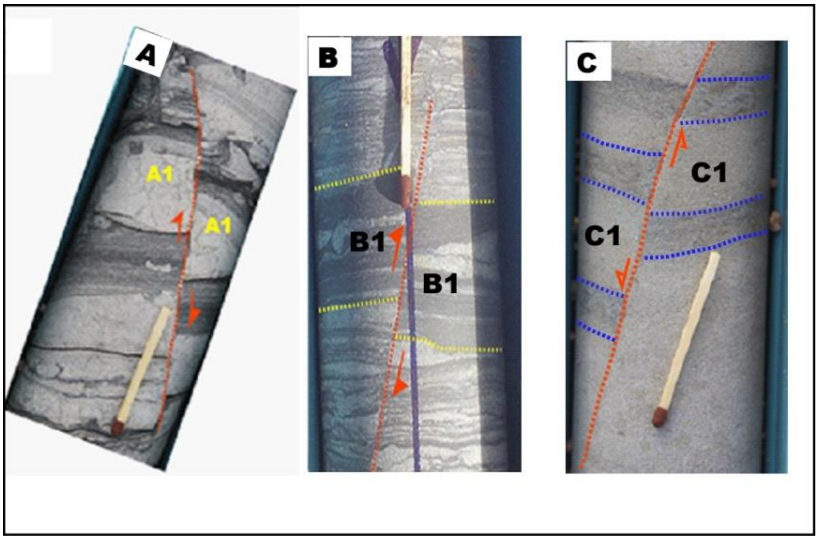

Figure 9. Drill cores showing thickness variations on both sides of the fault planes ((A and B): in the Carboniferous formation of Tarat (medium greyish sandstone with lenses of organic matter) and (C): in the Jurassic formation of Tchirezrine 2 (medium to coarse-grained greyish sandstone)).

deposits are affected by normal microfaults. These determine a microhorst and micrograben structure (Figure 8). Locally, the mirrors of these microfaults have mostly fluted or curved striations (Figure 7, location St2 and St3 in Figure 10). The normal microfaults N70° and N90° are sometimes shifted into sinistral by N140° strike-slip microfaults. The thickness and facies variations on both sides of these microfaults show their syn-sedimentary character. Figure 9 (A and B) reveals a syn-sedimentary reverse microfault affecting Carboniferous deposits while

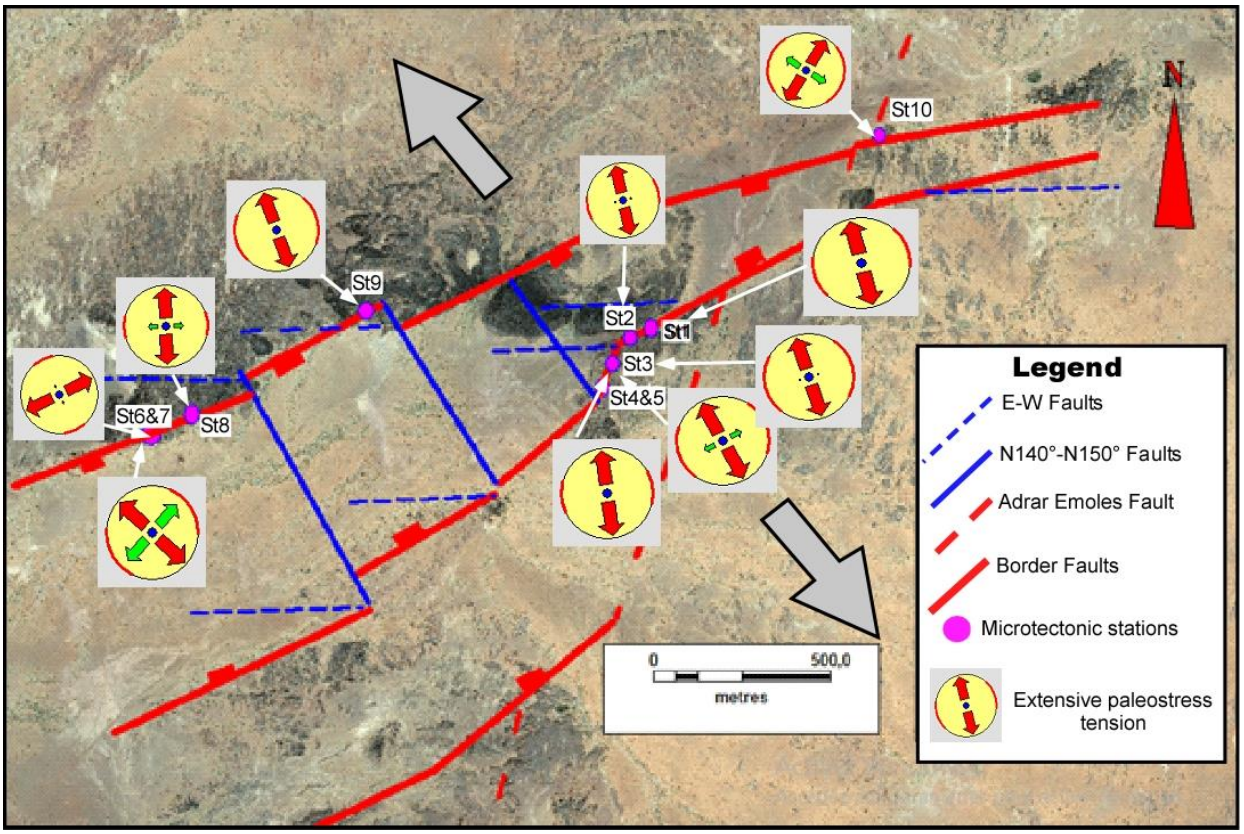

Figure 10. Map of distribution of stress tensors related to the Jurassic-Cretaceous tectonic phase and average direction of extension.

Figure 9 (C) displays a syn-sedimentary normal microfaults affecting the Jurassic deposits.

The only outcropping deposits on the border of the DASA graben are Jurassic in age. The Lower Cretaceous deposits composed mainly of the Irhazer shales are not observable in outcrop. The syn-deposition microfaults observed on the outcrops give indications of the episode of synchronous deformation of the Jurassic deposits, which were affected after their establishment by a second post-deposition deformation phase. The generated structures include abrasion or cataclase features (Riedel fractures, secondary synthetic fracture, spoon-shaped depression and syn-kinematic recrystallizations of silica.

The tectono-sedimentary analysis of the Lower Cretaceous infilling was derived from borehole and well log data. Microtectonic analysis is carried out onto the brittle faulting zone or semi-ductile deformation areas which are bordering the graben and where the tectonic structures are best preserved. This analysis is based on ten stations (St1 to St10) of microfault populations distributed across the Jurassic terrains. About 136 brittles to syn-deposition microfaults were considered (Figure 10).

Beside the outcrop, the syn-depositional character of the microfaults can be recognized by the following characters:

1. the microfault planes have the same color as the sediment patina (Figure 7);
2. the striae are linear or curved (Figure 7);
3. the faults planes are generally curved (Figure 7).

The post-deposition deformations that affected the graben after the Lower Cretaceous period is not considered.

Jurassic syn-deposition paleostress analysis

To study the dynamics of syn-depositions microfaults, the different populations of microfault planes were projected onto Win tensor program (Version win_tensor_5.8.9) of Damien Delvaux (2019). Automatic processing result of different striaes from populations of microfaults of the stations n°1, 2, 3, 4, 5, 6, 7, 8, 9 and 10 shows evidence of extensional paleostress tensors (Figure 10).

The obtained extensional paleostress tensors were plotted onto the map of the DASA area. Each tensor is represented by a pellet characterized by the number of the station reference and the direction of the minimum stress σ_3 (Figure 10).

At the scale of the DASA graben, the processing of the

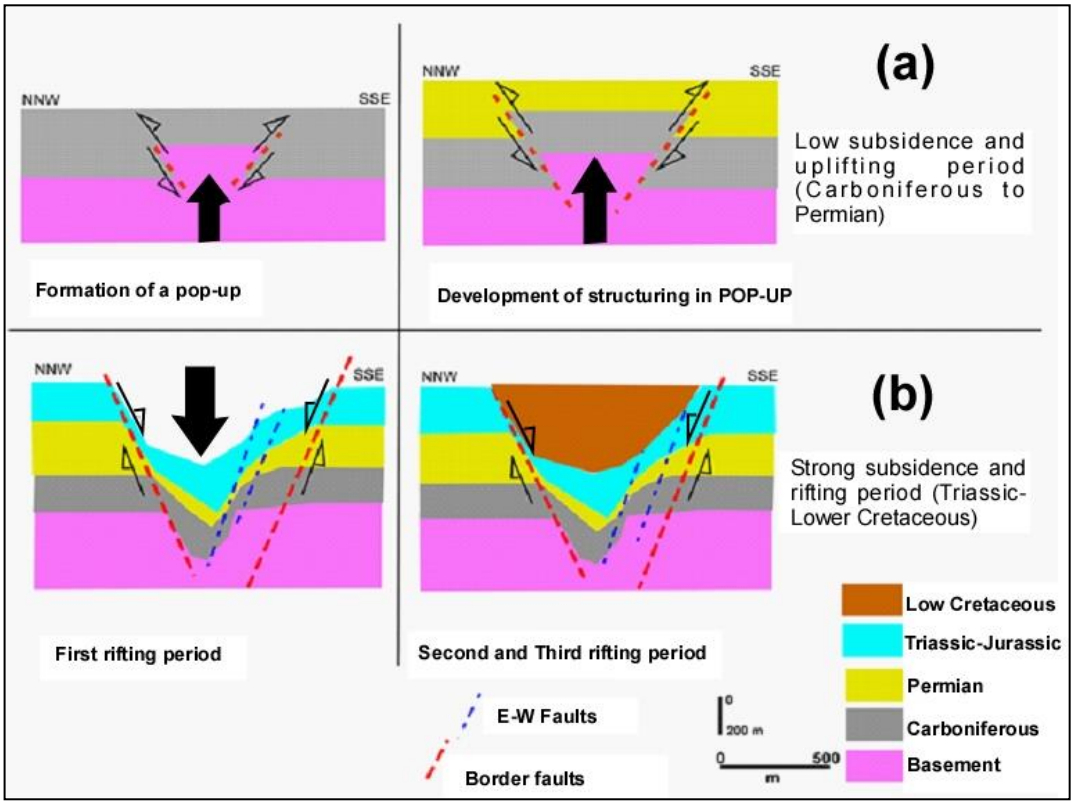

Figure 11. DASA graben Model Evolution at Carboniferous to Lower Cretaceous.

different populations of pre-deposition microfaults made it possible to distinguish three types of extensive paleostress tensors:

1. extensive paleostress tensors with σ_3 varying from N130° to N170° (St1, 2, 3, 4, 5, 8 and 9);
2. extensive paleostress tensors with σ_3 varying from N30° to N70° (St6 and 10);
3. radial extensive paleostress tensors (St7).

The paleostress tensors distribution map shows a large variation in the direction of the minimum stress σ_3 (Figure 10). During the Jurassic period, the study area underwent a N160° extensional phase which allowed the opening of the DASA graben.

DISCUSSION

The tectono-sedimentary evolution of the DASA graben is the result of the interaction between an uplift phase (from the Carboniferous to the Permian) and a rifting phase (from the Triassic to the Lower Cretaceous). The uplift period highlighted in the DASA graben shows that at least one compression period affected the region during the Late Paleozoic. The rifting phases, which occurred from the Triassic to the Lower Cretaceous, imply that the region was subjected to a period of distension (Figures 11 and 12). To explain the succession of these two phases of structuring (uplift/rifting) over the time, the results of this study are compared to those realized in other African basins, such as Tim Mersoï, Téfidet (North Niger), Benue trough (Nigeria) and Muglad basin (Sudan).

According to the literature data, a N40° visean compression phase has been highlighted in Algeria in the area of Ougarta by Blès (1969), in the Béchar Basin by Conrad and Lemosquet (1984), in the Illizi Basin by Boudjema (1987) and in the Ahnet Basin by Zazoun (2001). In the Tim Mersoï basin too, a N25° horizontal shortening, upper Visean in age was highlighted by Konaté et al. (2007). During this Visean episode of shortening, the N70° trending Tin Adrar fault system was reactivated as a strike-slip fault.

The uplift observed in the DASA graben, during the Upper Paleozoic, indicates that the strike-slip sinistral reactivation of the N70° trending faults has a reverse component. At that time, a transpressive tectonic regime would have affected the DASA graben. This could explain the fact that the thicknesses of the Upper Paleozoic series are thinner in the axial zone and corresponded to a paleo-high with respect to the bordering zones, which had collapsed and showed higher thicknesses. The DASA

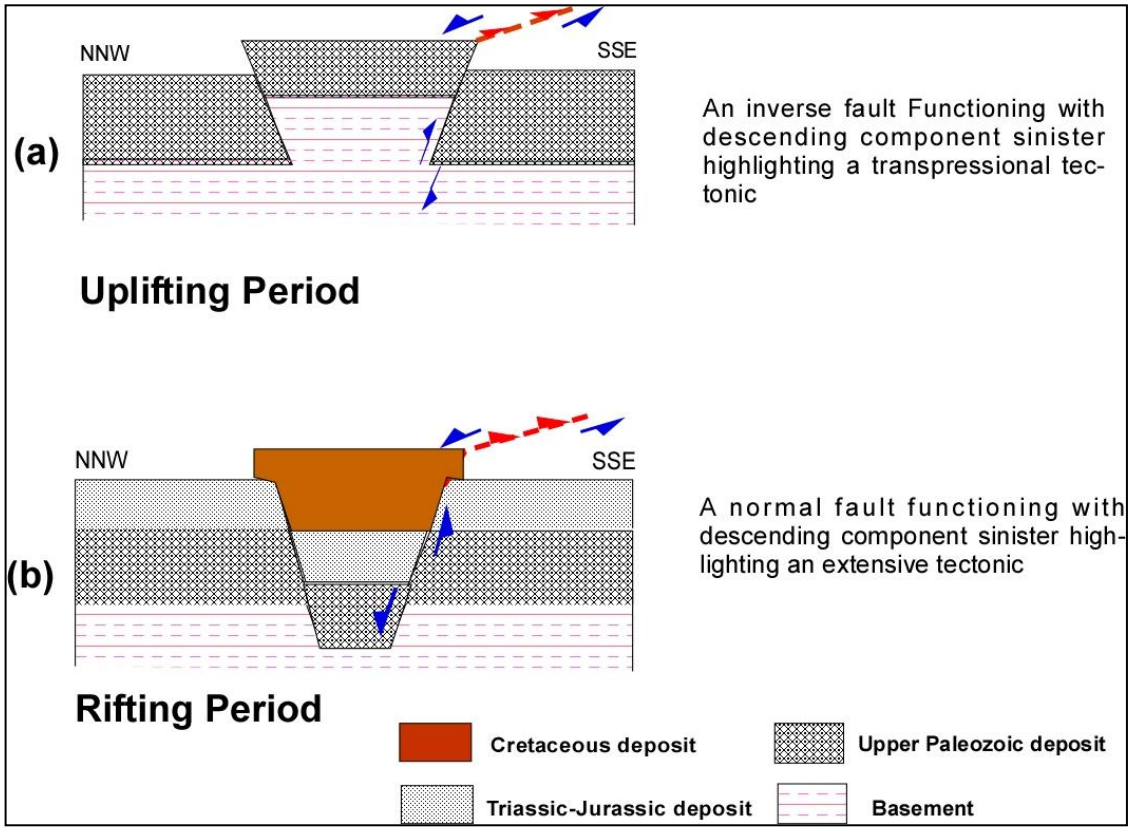

Figure 12. Geodynamic evolution of the DASA graben showing an inversion of the tectonic regime. A. Uplifting period, B. Rifting period.

graben shows a relatively low sedimentation rate in the axial zone (1.67 m/Ma), compared to the border zones (3.65 to 3.75 m/Ma) during the Upper Paleozoic period. These observations are in agreement with the prevailing uplift episode.

The second structuring period of the DASA graben is marked by a change in the tectonic regime (Figures 11 and 12). This is characterized by a rifting phase preserved over a long period from the Triassic to the Lower Cretaceous.

The structural evolution of the DASA graben during the Jurassic-Cretaceous period is compared to those of the West and Central African Rift Systems, commonly referred to as WCARS. During the Lower Cretaceous, these rift systems were affected by extensive to transtensive tectonics regime (Guiraud, 1993, Ye, 2016), favoring a strong subsidence, 54 m/Ma for the Termit basin (Liu et al., 2015), 65 m/Ma for the Muglad Basin (Yassin., 2016), 43 m/Ma for the Benue trough (Guiraud and Maurin, 1992) and 13 m/Ma for the Téfidet trough (Konaté et al., 2019).

Unlike those Cretaceous rift systems, the DASA graben has a lower subsidence rate (6.52 m/Ma). Given the geodynamic context during the Cretaceous, these extensional tectonics regimes affecting the DASA graben could be associated to the opening of the South Atlantic occurring during that period (Genik., 1992, Guiraud et al., 2005, Ye, 2016). The structural evolution of the DASA graben is marked by tectonics inversion (Figures 11 and 12).

Conclusion

This study has integrated field geology, cartography, well log, microtectonics, tectono-sedimentary analysis and shows that the evolution of the DASA graben is closely related to the polyphase kinematics of the N70° border faults. The sedimentological and structural characteristics of the DASA graben (e.g., non-homogeneity of the main stresses, stratigraphic gaps, and mismatch in the vertical facies sequence) characterize a particular type of basin evolving from an Upper Paleozoic transpressive regime to an extensive Mesozoic regime (Figure 12). The strong subsidence observed within the Lower Cretaceous in the DASA graben could be related to the initial stages of opening of the Atlantic Ocean. After the rifting phase, the DASA graben was affected by a post-cretaceous compressive phase related to the collision between Africa and Europe.

CONFLICT OF INTEREST

The authors declare that they have no conflict of interest.

ACKNOWLEDGEMENTS

The authors are grateful to and acknowledge the efforts of the staff of Global Atomic Corporation for their collaboration. The authors are particularly grateful to Mr. Stephan Roman, George Flach and Abdoulaye Din Christophe of Global Atomic Corporation for their technical and material support.

REFERENCES

Billon, S. (2014). Minéraux argileux dans le gisement uranifère d'Imouraren (Bassin de Tim Mersoï, Niger): Implications sur la genèse du gisement et sur l'optimisation des processus de traitement du minerai. Thèse Terre solide et enveloppes superficielles. Poitiers: Université de Poitiers, 2014.

Blès, J. L. (1969). Les relations des microfractures avec le plissement dans la région du Djebel Ben Tadjine et au 'km 30' (Chaînes d'Ougarta-Sahara occidental, Algérie). *Publication Service Géologique Algérie* 39,193-204.

Boudjema, A. (1987). Évolution structurale du bassin pétrolier 'triasique' du Sahara Nord Oriental (Algérie). Thèse Doctorat Etat, Paris XI-Orsay, France, 290p.

Cazoulat, M. (1985). Geologic environment of the uranium deposits in the Carboniferous and Jurassic sandstones of the Western margin of the Aïr mountains in the Republic of Niger. In: *Geological environments of sandstone-type uranium deposits*. IAEA-TECDOC 328, Vienna, Pp.247-263.

Clermonté, J., Yahaya, M., Lang, J., & Oumarou, J. (1991). Un bassin paléozoïque et mésozoïque dans une zone en décrochement: le Tim Mersoï dans la région d'Arlit, à l'Ouest de l'Aïr (Niger). *Comptes rendus de l'Académie des sciences. Série 2, Mécanique, Physique, Chimie, Sciences de l'univers, Sciences de la Terre*, 312(10), 1189-1195.

Conrad, J., & Lemosquet, Y. (1984). Du craton vers sa marge; evolution sedimentaire et structurale du bassin Ahnet-Timimoun-Bechar (Sahara algerien) au cours du Carbonifere; donnees paleoclimatiques. *Bulletin de la Société Géologique de France*, 7(6), 987-994.

Damien, D. (2019). Tensor program fault-kinematic analysis and tectonic stress tensor inversion. Version: Win-tensor_5-8-9. Retrieved from http://damiendelvaux.be/Tensor/WinTensor/win-tensor.html

El hamet, M. O. (1983). Analyse géologique et pétrographique de la formation de Tarat dans les carrières Somaïr (Paléozoïque supérieur). Essai d'interprétation paléoclimatique à la lumière de l'épisode glaciaire dévono-carbonifère (Région d'Arlit – Niger septentrional) [PhD. thesis] : Université de Dijon (France) et Université de Niamey (Niger), 279p.

Forbes, P. (1989). Rôles des structures sédimentaires et tectoniques, du volcanisme alcalin régional et des fluides diagénétiques-hydrothermaux pour la formation des minéralisations à U-Zr- Zn-V-Mo d'Akouta (Niger): mémoire édité par le Centre de Recherches sur la Géologie de l'Uranium (CREGU), Nancy, 376p.

Genik, G. J. (1992). Regional framework, structural and petroleum aspects of rift basins in Niger, Chad and the Central African Republic (CAR). *Tectonophysics*, 213(1-2), 169-185.

Gerbeaud, O. (2006). Evolution structurale du Bassin de Tim Mersoï : Déformations de la couverture sédimentaire, Relations avec la localisation des gisements d'uranium du secteur d'Arlit (Niger). Thèse de doctorat Université de Paris-Sud UFR scientifique d'Orsay, 270p.

Greigert, J., & Pougnet, R. (1967). Essai de description des formations géologiques de la République du Niger : Paris, Editions du BRGM, 273 pages.

Guiraud, M. (1993). Late Jurassic rifting-early Cretaceous rifting and late Cretaceous transpressional inversion in the upper Benue basin (NE Nigeria). *Bulletin des centres de recherches exploration-Production Elf-Aquitaine*, 17(2), 371-383.

Guiraud, R., & Maurin, J. C. (1992). Early Cretaceous rifts of Western and Central Africa: an overview. *Tectonophysics*, 213(1-2), 153-168.

Guiraud, R., Bosworth, W., Thierry, J., & Delplanque, A. (2005). Phanerozoic geological evolution of Northern and Central Africa: an overview. *Journal of African Earth Sciences*, 43(1-3), 83-143.

Guiraud, R., Boureïma O., & Robert J. P. (1981). Mise en évidence de déformations traduisant un raccourcissement dans le Mésozoïque de la périphérie de l'Aïr (Niger). *Comptes-Rendus Académie des Sciences*, 292(9), 753-756.

Joulia, F. (1959). Les series primaires au N et NW de l'Air (Sahara central); discordances observees. *Bulletin de la Société Géologique de France*, 7(2), 192-196.

Joulia, F. (1963). Carte géologique de reconnaissance de la bordure sédimentaire occidentale de l'Aïr au 1/500 000. Éditions du BRGM, Orléans, France.

Konaté, M., Ahmed, Y., & Harouna, M. (2019). Structural evolution of the Téfidet trough (East Aïr, Niger) in relation with the West African Cretaceous and Paleogene rifting and compression episodes. *Comptes Rendus Geoscience*, 351(5), 355-365.

Konate, M., Denis, M., Yahaya, M., & Guiraud, M. (2007). Structuration extensive au devono-dinantien du bassin de Tim Mersoı (Bordure occidentale de l'Aır, Nord Niger): Université de Ouagadougou. *Annales, Série C*, *5*, 32.

Liu, B., Wan, L., Mao, F., Liu, J., Lü, M., & Wang, Y. (2015). Hydrocarbon potential of Upper Cretaceous marine source rocks in the Termit Basin, Niger. *Journal of Petroleum Geology*, 38(2), 157-175.

Mamadou, M. M. (2016). *Le système métallogénique des gisements d'uranium associés à la faille d'Arlit (Bassin de Tim Mersoï, Niger): diagenèse, circulations des fluides et mécanismes d'enrichissement en métaux (U, Cu, V)* (Doctoral dissertation, Université de Lorraine, 402 pages).

Moussa, Y. (1992). *Dynamique sédimentaire du Guézouman et des formations viséennes sous-jacentes en liaison avec la tectonique, le volcanisme et le climat, paléomilieux des gîtes uranifères d'Arlit (Niger)*. Thèse Doctorat troisième cycle, Université de Dijon, 357 pages.

Sempéré, T. (1981). *Le contexte sédimentaire du gisement d'uranium d'Arlit (République du Niger)*. Thèse de doctorat, ENSMP, Paris, 382 pages.

Tauzin, P. (1981). Cadre géologique des gisements d'uranium de la bordure orientale du bassin sédimentaire du Tim Mersoï.

Rapport interne Minatome, 15 pages.
Valsardieu, C. 1971. *Etude géologique et paléogéographique du bassin de Tim Mersoï, région d'Agadès (République du Niger)*. Thèse de doctorat, université de Nice, 518 pages.
Wagani, I. (2007). Potentialités uranifères des sources volcaniques envisageables pour la formation des minéralisations de la région d'Arlit (Niger). Thèse de l'université de Paris Sud, 291 pages.
Wright, L. (1989). Etude du bassin houiller d'Anou Araren - Solomi, Phase 1 : Etude des données ; Charbon de l'Aïr, Charbonnages de France avec British Mining Consultants Ud., Pp. 21-51.
Yassin, M. A., Hariri, M. M., Abdullatif, O. M., Korvin, G., & Makkawi, M. (2017). Evolution history of transtensional pull-apart, oblique rift basin and its implication on hydrocarbon exploration: A case study from Sufyan Sub-basin, Muglad Basin, Sudan. *Marine and Petroleum Geology*, 79, 282-299.
Ye, J. (2016). *Evolution topographique, tectonique et sédimentaire syn-à post-rift de la marge transformante ouest Africaine* (Doctoral dissertation, Université de Toulouse, Université Toulouse III-Paul Sabatier).
Zazoun, R. S. (2001). La tectogenese hercynienne dans la partie occidentale du bassin de l'Ahnet et la region de Bled El-Mass, Sahara Algerien: un continuum de deformation. *Journal of African Earth Sciences*, 32(4), 869-887.